

# Onset of convection in fluids with strongly temperature-dependent, power-law viscosity:

## 2. Dependence on the initial perturbation

V.S. Solomatov<sup>a,\*</sup> and A.C. Barr<sup>b</sup>

<sup>a</sup>*Department of Earth and Planetary Sciences, Washington University in St. Louis, St. Louis, MO 63130, USA*

<sup>b</sup>*Department of Space Studies, Southwest Research Institute, Boulder, CO, 80302, USA*

---

### Abstract

Starting convection in the power-law creep regime on the silicate and icy planetary bodies requires a finite amplitude initial perturbation. The requirement for a finite-amplitude perturbation raises an important question: How large does the perturbation have to be to cause convection? Because the problem is highly nonlinear, both the amplitude and shape of the optimal perturbation for starting convection is important. Here we suggest some preliminary constraints on how the critical Rayleigh number depends on the amplitude and form of temperature perturbation issued to an initially conductive two-dimensional horizontal fluid layer with a fixed temperature contrast between the boundaries. At Rayleigh numbers much larger than the absolute minimum critical Rayleigh number,  $Ra_{cr}^*$  (the Rayleigh number below which all perturbations decay regardless of their amplitude) the critical perturbation necessary to initiate convection is  $\delta T_{cr} \sim (RT^2/E)(Ra_{cr}^*/Ra)^{n/(n-1)}$  where  $RT^2/E$  is the rheological temperature scale,  $E$  is the activation energy, and

$T$  is the temperature at the base of the layer. A perturbation of this amplitude has to be located in the rheological sublayer – in the least viscous region located at the base of the layer. The wavelength of most efficient perturbations scales with the thickness of the rheological sublayer.

*Key words:* Dislocation creep, Power-law viscosity, Convection

---

## 1 Introduction

Understanding the conditions for the onset of convection in fluids with complicated rheologies is essential for models of the dynamics and evolution of planetary interiors. This information is necessary to address long-standing questions about the interiors of terrestrial planets and icy satellites: Does convection occur beneath the lithospheres of the terrestrial planets and icy satellites (Schubert et al. 1969; Reynolds and Cassen 1979; McKinnon 1999; Solomatov and Moresi 2000; Barr et al. 2004; Barr and Pappalardo 2005)? Do small-scale instabilities occur beneath continents and oceans on Earth (Davaille and Jaupart 1993; Korenaga and Jordan 1993; Lenardic and Moresi 1999; Sleep 2005) and at the base of the mantle (Solomatov and Moresi 2002)?

Although the onset of convection in constant viscosity fluids (Chandrasekhar 1962) and in temperature-dependent viscosity fluids (Stengel et al. 1982; Solomatov and Barr 2006, 2007) has been well-studied, the onset of convection in power-law viscosity fluids where dislocation creep and/or grain boundary sliding accommodate strain, is not well-understood. The dislocation creep is a

---

\* Corresponding author.

*Email address:* [slava@wustl.edu](mailto:slava@wustl.edu) (V.S. Solomatov).

strong competitor to diffusion creep in planetary mantles and it is not easy to draw the boundary between the two (e.g. Solomatov and Moresi 2000). The dislocation creep regime may dominate convective instabilities in silicate bodies if one takes into account grain growth which tends to suppress diffusion creep while has no effect on dislocation creep (Karato and Wu, 1993). In icy satellites, convective instability may be governed by weakly non-Newtonian grain boundary sliding if ice grain sizes exceed 1 mm (Barr and Pappalardo 2005; Barr and McKinnon 2006).

The linear onset of convection in the dislocation creep regime has been studied by Birger (1980, 2000). His solutions describe the onset of convection for infinitesimal amplitudes, when Andrade law is applicable. At large amplitudes one needs to consider power-law rheology. The main difficulty of this problem is that this is a finite-amplitude instability – the viscosity tends to infinity for infinitesimal-amplitude perturbations. It is hard to see how one can avoid this singularity. Even if the initial stage is described by a transient creep law (such as Andrade law), after about 10% of deformation, the creep is in a steady-state regime (from the point of view of dislocation dynamics) and one has to investigate how the flow will evolve after that. This issue was addressed in (Solomatov and Barr 2006), where we investigated the onset of convection in strongly temperature-dependent, power-law viscosity fluids for a layer with a fixed temperature difference between the boundaries. We calculated the absolute minimum critical Rayleigh number,  $Ra_{cr}^*$ , below which all perturbations decay independently of the amplitude. Although it is useful to know when convection does not occur, it may be more important to know when it does occur. This is a more difficult problem because both the amplitude and shape of the perturbations play a large role. This problem has many similarities with

other problems in nonlinear fluid dynamics such as transition to turbulence (Landau and Lifshitz 1987).

## 2 Model

We use equations of thermal convection in the Boussinesq approximation. We study convection in an  $a \times 1$  box with free-slip boundaries. The temperature of the upper boundary  $T = 0$  and the temperature of the lower boundary  $T = 1$ . The viscosity is temperature and stress dependent,

$$\eta = b\tau^{1-n} \exp(-\gamma T) \quad (1)$$

where  $\tau$  is the second invariant of the stress tensor,  $n$  is the stress exponent, and  $\gamma$  controls the variation of viscosity due to temperature alone, and can be related to the activation energy in the laboratory-derived creep law (e.g. Solomatov and Moresi, 2000).

The problem is characterized by two non-dimensional parameters: the viscosity contrast due to temperature alone,

$$\Delta\eta = \exp(\theta) \quad (2)$$

and the Rayleigh number

$$Ra = \frac{\alpha g \rho \Delta T d^{(n+2)/n}}{\kappa^{1/n} b^{1/n}}, \quad (3)$$

where  $\theta = \gamma^{-1} \Delta T$ ,  $\Delta T$  is the temperature difference between the boundaries, and  $d$  is the thickness of the convective layer. Typical values are  $\Delta\eta \approx 10^6 - 10^{16}$  (Solomatov and Moresi 1997; Barr et al. 2004).

The Nusselt number, which describes the nondimensional convective heat flux, is defined as

$$Nu = \frac{Fd}{k\Delta T} \quad (4)$$

where  $F$  is the heat flux,  $k = \rho c_p \kappa$  is the thermal conductivity, and  $c_p$  is the isobaric specific heat. When convection occurs,  $Nu > 1$ ,  $Nu = 1$  indicates no convection, and  $Nu \sim 1$  indicates sluggish convection.

We perform simulations of convection using the finite element model CITCOM (Moresi and Solomatov 1995). We generally use  $m = 64$  vertical elements and vary the number of elements in the horizontal direction (which has variable width  $a$  – the aspect ratio) to keep the elements approximately square. We perform a few simulations with  $m = 128$  and estimate that the errors due to numerical resolution are  $< 1\%$ .

### 3 Perturbation function

We will take the advantage of the main physical feature of convection at large viscosity contrasts (stagnant lid regime) – that convection is confined to the rheological sublayer at the bottom.

First, it is clear that perturbations located outside of the rheological sublayer, that is in the stagnant lid, do not help drive convective motion because they quickly diffuse away. To be effective, the perturbation has to be localized in the rheological sublayer. The most effective perturbation can be constructed using the solution at the critical point,  $Ra = Ra_{\text{cr}}^*$ , where a steady finite-amplitude solution exists. At  $Ra < Ra_{\text{cr}}^*$  all convective motions eventually

decay regardless of the initial condition.

The solution at  $Ra = Ra_{\text{cr}}^*$  has all the essential features for an optimal temperature perturbation function: the temperature perturbation is largest in the rheological sublayer and disappears in the stagnant lid. This is probably the most energetically efficient perturbation that one can possibly construct. Thus, a perturbation can be constructed from the temperature field of the convecting fluid with  $a = a_{\text{cr}}^*$ ,  $Ra = Ra_{\text{cr}}^*$  as

$$T_o(x, y) = T_{\text{cond}} + \xi(T_{\text{cr}}^*(x, y) - y) \quad (5)$$

where  $T_{\text{cr}}^*(x, y)$  is the temperature field at the critical point and  $\xi$  is the perturbation amplitude. When  $\xi = 0$ , the initial temperature field is purely conductive. When  $\xi = 1$ , the initial temperature field is identical to the solution at  $a = a_{\text{cr}}^*$  and  $Ra_{\text{cr}}^*$ , which yields  $Nu_{\text{cr}}^*$ .

For a given perturbation amplitude,  $\xi < 1$ , one can find the critical Rayleigh number,  $Ra_{\text{cr}}(\xi)$  at which the system becomes unstable.

An example of calculations of the critical Rayleigh number for  $n = 3$  and  $\exp(\theta) = 10^{10}$  is shown in Figure (1). The results are presented in  $Ra - Nu$  axes rather than  $Ra - \xi$ . The Nusselt number of steady-state solutions is calculated from Eq. (4). The Nusselt number corresponding to a perturbation with  $\xi < 1$  is related to  $\xi$  as

$$Nu(\xi) = 1 + \xi(Nu_{\text{cr}}^* - 1). \quad (6)$$

The meaning of the Nusselt number calculated by Eq. (6) is that this is the initial Nusselt number of the convective flow caused by the perturbation of

amplitude  $\xi$ . If  $Ra < Ra_{\text{cr}}(\xi)$ , then the perturbation will decay and the Nusselt number will decrease from  $Nu = Nu(\xi)$  to  $Nu = 1$ . If  $Ra > Ra_{\text{cr}}(\xi)$ , then the perturbation will grow and reach a finite-amplitude solution with  $Nu > Nu(\xi)$ .

Theoretically, there must exist an exact temperature field and the corresponding convective flow such that at  $Ra = Ra_{\text{cr}}(\xi)$  the flow is steady, that is  $\partial T/\partial t = 0$  everywhere. In the absence of any perturbations, it would persist indefinitely but would become unstable to infinitesimal perturbations - it would either decay or grow. These solutions constitute the so-called unstable branch (Busse 1967; Palm 1975; Drazin and Reid 1981) and can be plotted on the same diagram in the  $Nu - Ra$  axes.

Although the exact calculation of the unstable branch is beyond the scope of this paper, the function  $Nu(Ra_{\text{cr}})$  calculated by Eq. (6) gives some idea of how the actual unstable branch looks like. A similar type of calculations give a reasonable approximation for the unstable branch for  $n = 1$  (Solomatov and Barr 2007). From the point of view of nonlinear dynamics, the diagram shown in Fig. 1 is a bifurcation diagram. The critical point at  $Ra = Ra_{\text{cr}}^*$  is called a saddle-node bifurcation.

### *3.1 Comparison of perturbation functions*

Although the special perturbations constructed using the critical solution are the most efficient ones, it is interesting to explore how the onset of convection depends on the shape of the perturbation. Below we conduct a simple test in which we compare the critical Rayleigh numbers for different initial

perturbations for the case  $n = 3$ ,  $\exp(\theta) = 10^{20}$ .

First, a reference perturbation is constructed as usual: we take the near-critical stable solution for  $n = 3$  and  $\exp(\theta) = 10^{20}$  and reduce the temperature anomaly of the near-critical convective solution by a factor of  $\xi = 0.1$  (Eq. 5).

A different type of perturbation may be constructed using a trigonometric function

$$\delta T_{\text{sin}} = \delta T_0 \sin(0.5\pi x/a) \sin[\pi(y - y_b)/(y_t - y_b)] \quad (7)$$

which is confined within a sublayer  $y_t < y < y_b$ . The perturbation is zero outside of this sublayer. This perturbation is added to the conductive temperature profile  $T_{\text{cond}} = y$ :

$$T_{\text{sin}} = T_{\text{cond}} + \delta T_{\text{sin}}. \quad (8)$$

The amplitude  $\delta T_0$  is adjusted so that it matches the amplitude of the reference perturbation.

Experiments with various initial conditions (Fig. 2) show that the shape of the perturbation is not very important provided the perturbation is located within the rheological sublayer. Perturbations in the stagnant part of the layer are very ineffective in driving fluid motion. Starting convection from temperature fluctuations localized in the stagnant lid may require perturbation amplitudes and/or Rayleigh numbers orders of magnitude larger than a similar-amplitude perturbation located in the rheological sublayer. In the case of an arbitrary perturbation, the onset of convection will depend on whether or not the initial perturbation will diffuse into the rheological sublayer and will have a

sufficiently large amplitude in the rheological sublayer.

### 3.2 Results

First, we reached the lowest possible Rayleigh number at which steady-state convection still exists and estimated the parameters at the critical point using parabolic functions in the vicinity of the critical point (Fig. 1). This gives us the absolute minimum critical Rayleigh number,  $Ra_{\text{cr}}^*$ , and the corresponding Nusselt number,  $Nu_{\text{cr}}^*$ . We also calculated the maximum amplitude of lateral temperature variation,  $\delta T_{\text{cr}}^*$ , which we use as a measure of the perturbation amplitude.

Second, we calculated the critical Rayleigh number for the onset of convection as a function of perturbation amplitude,  $\xi$ , using the perturbation function from the critical solution at  $Ra = Ra_{\text{cr}}^*$ , as described above. The results are summarized in Table 1 and Fig. 4.

## 4 Criterion for finite amplitude instabilities

### 4.1 Scaling analysis

Numerical simulations show that when the initial perturbation,  $\delta T$ , is imposed on the system, the flow grows or decays very quickly (unless  $\delta T$  is very close to the critical value). This means that the viscosity and the Rayleigh number based on the effective initial stress

$$\tau_{\text{eff}} \sim \alpha \rho g \delta T d_{\text{sub}} \tag{9}$$

can be used to predict the onset of convection.

Following Stengel et al. (1982) and Solomatov (1995), we determine this Rayleigh number at the mean temperature of the rheological sublayer of thickness  $d_{\text{rh}}$  and the effective stress (9):

$$Ra_{\text{sub}} = \left\{ \frac{\alpha \rho g (dT/dy) d_{\text{sub}}^4}{\kappa b \tau_{\text{eff}}^{1-n} \exp[-\theta(1 - d_{\text{sub}}/2d)]} \right\}^{1/n}, \quad (10)$$

where  $dT/dy = \Delta T/d$  is the temperature gradient in the layer. Although it is not important here, we used the power  $1/n$  to ensure that this Rayleigh number is reduced to the usual one when  $\tau = \alpha \rho g (dT/dy) d_{\text{sub}}^2$ .

The requirement  $\partial Ra_{\text{sub}}/\partial d_{\text{sub}} = 0$  gives the thickness  $d_{\text{sub}}$  of the rheological sublayer and the temperature difference  $\Delta T_{\text{sub}}$  across the rheological sublayer:

$$d_{\text{sub}} = 2(n+3)\theta^{-1}d, \quad (11)$$

$$\Delta T_{\text{sub}} = 2(n+3)\theta^{-1}\Delta T. \quad (12)$$

Equation 11 gives us the thickness of the sublayer with the largest Rayleigh number (the most unstable sublayer). Putting the value of (11) back into Eq. (10) gives us the Rayleigh number for the sublayer. The onset of convection can be determined by requiring that this sublayer is at the boundary of convective stability:

$$Ra_{\text{sub}} = Ra_{\text{cr}}(n), \quad (13)$$

where  $Ra_{\text{cr}}(n)$  is the critical Rayleigh number for a fluid whose viscosity does not depend on temperature.

We obtain that the critical Rayleigh number is

$$Ra_{1,\text{cr}} = Ra_{\text{cr}}(n) \left[ \frac{\theta}{2(n+3)} \right]^{(n+3)/n} e^{(n+3)/n} \left[ \frac{\Delta T}{\delta T} \right]^{(n-1)/n}. \quad (14)$$

or

$$Ra_{1,\text{cr}} = Ra_{\text{cr}}(n) \left[ \frac{\theta}{2(n+3)} \right]^{2(n+1)/n} e^{(n+3)/n} \left[ \frac{\Delta T_{\text{sub}}}{\delta T} \right]^{(n-1)/n}. \quad (15)$$

Equation (15) gives the desired dependence of the Rayleigh number on the amplitude of the perturbation. It is applicable for small perturbation amplitudes and cannot be applied at large perturbations,  $\Delta T \sim \Delta T_{\text{sub}}$ , that is near the critical point where the function should become parabolic. At  $\Delta T > \Delta T_{\text{sub}}$  the perturbation amplitude does not matter any more – the critical Rayleigh number cannot be smaller than the absolute minimum critical Rayleigh number,  $Ra_{\text{cr}}^*$  (as noticed by Barr et al. 2004).

#### 4.2 A criterion for the onset of convection

To obtain a criterion for the onset of convection by finite-amplitude perturbations, first we find a scaling law for  $\delta T_{\text{cr}}^*$ . Figure 3 shows that the amplitude of lateral temperature variations scales very well with the rheological temperature scale (12):

$$\delta T_{\text{cr}}^* = 0.9(n+3)\theta^{-1}. \quad (16)$$

The boundary  $Ra(\delta T)$  for the onset of convection can now be described by combining this equation with the results in Figure 4.

At  $Ra/Ra_{\text{cr}}^* > 3$ , the scaling formula obtained in the previous section compresses the data reasonably well (Fig. 4):

$$\frac{Ra}{Ra_{\text{cr}}^*} \approx 2.5 \left( \frac{\delta T_{\text{cr}}^*}{\delta T} \right)^{(n-1)/n}, \quad Ra > 3Ra_{\text{cr}}^*. \quad (17)$$

In the range between  $Ra = Ra_{\text{cr}}^*$  and  $\sim 3Ra_{\text{cr}}^*$  the temperature perturbation required to initiate convection is roughly

$$\frac{Ra}{Ra_{\text{cr}}^*} \approx \frac{\delta T_{\text{cr}}^*}{\delta T}, \quad Ra < 3Ra_{\text{cr}}^*, \quad (18)$$

where  $Ra_{\text{cr}}^*$  is the absolute minimum critical Rayleigh number.

### 4.3 Absolute minimum critical Rayleigh number

The absolute minimum critical Rayleigh number was estimated by Solomatov (1995) in the limit of large viscosity contrasts:

$$Ra_{\text{cr,th}}^* = Ra_{\text{cr}}(n) \left[ \frac{e\theta}{4(n+1)} \right]^{2(n+1)/n} \exp(-\theta/n) \quad (19)$$

where  $Ra_{\text{cr}}(n) = Ra_{\text{cr}}(1)^{1/n} Ra_{\text{cr}}(\infty)^{(n-1)/n}$ ,  $Ra_{\text{cr}}(1) = 1568$ , and  $Ra_{\text{cr}}(\infty) = 20$ .

Numerical calculations by Solomatov and Barr (2006) showed that this formula is accurate only within a factor of 2. It is unclear whether there is a simple power-law scaling for  $Ra_{\text{cr}}^*$ . The following formula seems to provide a good interpolation for data from  $n = 2$  to 4 and in the range between  $\exp(\theta) = 10^{10}$  and  $10^{40}$  (Table 1 and Fig. 5):

$$Ra_{\text{cr}}^* = (n+1)\theta^{-0.3} Ra_{\text{cr,th}}^*. \quad (20)$$

Note that the slope systematically decreases with  $\theta$  for all  $n$ , so the coefficient 0.3 in the above formula is an average value in the range between  $\exp(\theta) = 10^{10}$  and  $10^{40}$ . Also, the case  $n = 1$  is noticeably different from  $n > 1$  and is not accurately described by the above formula. This might be related to fundamental differences between  $n = 1$  and  $n > 1$ . For  $n = 1$ , the existence of hysteresis (the difference between the absolute critical Rayleigh number  $Ra_{cr}^*$  for cessation of convection and the critical Rayleigh number for the onset of convection by infinitesimal perturbations) or in nonlinear dynamics terminology, the saddle-node bifurcation, is solely due to the temperature-dependent viscosity. For  $n > 1$ , the critical Rayleigh number for the onset of convection by infinitesimal perturbations is infinity and the hysteresis (the saddle-node bifurcation) exists not only because of the temperature-dependent viscosity but also because of stress-dependence (Appendix A).

## 5 Discussion and conclusion

Unlike constant viscosity fluids where there is a single critical Rayleigh number for the onset of convection, whether convection occurs in fluids with variable viscosity can depend on the perturbation amplitude. In power-law viscosity fluids, initiation of convection is always a finite-amplitude instability. Solomatov and Barr (2006) estimated the absolute minimum critical Rayleigh number for the onset of convection in strongly temperature-dependent, power-law viscosity fluids. Here we addressed the question: How large does a finite-amplitude perturbation have to be to initiate convection in power-law viscosity fluids?

Temperature perturbations that are most effective at driving convective motion are located inside the rheological sublayer – in the portion of the fluid

layer where the viscosity is smallest. Perturbations with the lateral length scale of the order of the rheological sublayer thickness are most effective at starting convection. The onset of convection does not depend on the perturbation amplitude if the perturbations inside the rheological sublayer greater than or equal to  $\Delta T_{\text{cr}}^* = 0.9(n + 3)RT^2/E$ , where  $T$  is the temperature at the bottom of the layer and  $E$  is the activation energy.

For near-solidus silicates at near-solidus temperatures,  $\Delta T_{\text{cr}}^* \approx 300$  K (e.g. for  $T = 1700$  K and “wet” olivine rheology  $n = 3$  and  $E = 430$  kJ mol<sup>-1</sup>, Karato and Wu 1993). In terms of the effectiveness for initiation of convection, amplitudes larger than  $\Delta T_{\text{cr}}^*$  are equivalent to those with  $\delta T \sim \Delta T_{\text{cr}}^*$  because this is the maximum amplitude which can be sustained by convection. Perturbations with larger amplitudes will decay to  $\Delta T_{\text{cr}}^*$ . For  $\delta T \geq \Delta T_{\text{cr}}^*$  the absolute minimum critical Rayleigh number,  $Ra_{\text{cr}}^*$  can be used to predict the onset of convection. The value of  $Ra_{\text{cr}}^*$  was estimated by Solomatov (1995) and constrained numerically by Solomatov and Barr (2006) and this study, Eqs. (19, 20).

When the temperature perturbations are small ( $\delta T < \Delta T_{\text{cr}}^*$ ) the critical Rayleigh number  $\propto 1/\delta T$ . For example, a perturbation  $\delta T \sim 0.5\Delta T_{\text{cr}}^*$  will trigger convection when  $Ra \sim 2Ra_{\text{cr}}^*$ . This criterion can be used for perturbations as low as about  $\sim 0.3\Delta T_{\text{cr}}^* \sim 100$  K for power-law creep in silicates. The scaling law (17) gives the critical Rayleigh number in the limit of very small perturbations. For example, if the perturbations are only about 10 K, then the critical Rayleigh number for the onset of convection is  $\sim 20Ra_{\text{cr}}^*$ .

It may, in theory, possible to start convection in a fluid layer by imposing a perturbation outside of the rheological sublayer, that is in the stagnant

part of the layer. Such a situation may occur in planetary mantles whose surfaces are being warmed by impacts (e.g. Reese et al. 2002). In this case, the onset of convection can be substantially delayed because convection will only start when a temperature anomaly of sufficiently large amplitude (as discussed above) reaches the rheological sublayer by thermal diffusion.

Although we believe that this study has shed light upon the finite-amplitude onset of convection for power-law viscosity fluids, a comprehensive theory is yet to be developed. Recently-developed approaches employing energy methods have shown promise in addressing this type of problems (Capone and Gentile 1994).

## **Acknowledgments**

This work was supported by NASA.

## **Appendix A: Power-law viscosity without temperature dependence**

Here we show that onset of convection in power-law fluids requires a substantial finite amplitude perturbation even when the viscosity does not depend on temperature. This is in stark contrast with Newtonian fluids where the finite-amplitude onset of convection below the critical Rayleigh number predicted by linear theory is only due to temperature-dependent viscosity. Also, the calculations presented below can be compared with various laboratory experiments and previous numerical calculations, thus providing an additional test for our approach.

The results of calculations of the critical Rayleigh number for  $n = 1.1, 1.3, 2$  and  $3$  are shown in Fig. 6. These calculations are performed with rigid upper and lower boundaries to make a better comparison with previous studies. Also, earlier numerical studies were performed with  $a = 1$ , so we use  $a = 1$ . The comparison of cases with  $a = 0.9, 1$  and  $1.1$  showed that  $a = 1$  gives the maximum Nusselt number. Thus,  $a_{\text{cr}} \approx 1$ .

Our estimates of the critical Rayleigh number are higher than estimates obtained in previous work. The latest estimates were obtained by Ozoe and Churchill (1972) who had the highest values of the critical Rayleigh number but argued that their results are most accurate at the time. Yet, our results are slightly higher than even Ozoe and Churchill (1972), which may be due to several factors. First, Ozoe and Churchill (1972) used a much coarser grid than ours and extrapolated their results to a finer grid. Second, the Prandtl number in Ozoe and Churchill's (1972) calculations was  $\sim 10$  while in our calculation it is infinite. Finally, they found the critical Rayleigh number by extrapolating  $Nu(Ra)$  to  $Nu = 1$ , but it should be extrapolated to  $Nu = Nu_{\text{cr}}$  (Fig. 7).

## References

- [1] Barr, A. C., R. T. Pappalardo, S. Zhong, 2004. Convective instability in ice I with non-Newtonian rheology: Application to the icy Galilean satellites. *J. Geophys. Res.* 109, doi:10.1029/2004JE002296.
- [2] Barr, A. C., Pappalardo, R. T., 2005. Onset of convection in the icy Galilean satellites: Influence of rheology, *J. Geophys. Res.* 110, 10.1029/2004JE002371.
- [3] Barr, A. C., McKinnon, W. B. 2006. Convection in ice I shells and mantles with self-consistent grain size. *J. Geophys. Res.* *in press*.
- [4] Birger, B.I., 1980. Thermoconvective waves in the Earths mantle. *Phys.Earth Planet. Inter.* 22, 238-243.
- [5] Birger, B.I., 2000. Excitation of thermoconvective waves in the continental lithosphere. *Geophys. J.* 140, 24-36.
- [6] Busse, F.H., 1967. The stability of finite amplitude cellular convection and its relation to an extremum principle. *J. Fluid Mech.* 30, 625-649.
- [7] Carter, N.L., and Kirby, S.H., 1978. Transient creep and semibrittle behavior of crystalline rocks. *Pure Appl. Geophys.*, 116, 807-839.
- [8] Capone, F., Gentile, M. 1994. Nonlinear stability analysis of convection for fluids with exponentially temperature-dependent viscosity. *Acta Mech.* 107, 53-64.
- [9] Chandrasekhar, S., *Hydrodynamic and Hydromagnetic stability.* Oxford, pp. 654, 1961.
- [10] Davaille, A., Jaupart, C., 1994. Onset of thermal-convection in fluids with temperature-dependent viscosity: Application to the oceanic mantle, *J. Geophys. Res.* 99, 19853-19866.

- [11] Drazin, P. G., W. H. Reid, 1981. *Hydrodynamic stability*. Cambridge Univ. Press, New York.
- [12] Karato, S.-I., Wu, P., 1993. Rheology of the upper mantle: A synthesis. *Science* 260, 771-778.
- [13] Korenaga, J., Jordan, T. H., 2003. Physics of multiscale convection in Earth's mantle: Onset of sublithospheric convection. *J. Geophys. Res.* 108, 10.1029/2002JB001760.
- [14] Landau L. D., Lifshitz, E. M., 1987. *Fluid Mechanics*. Butterworth-Heinemann, pp. 552.
- [15] Lenardic, A., Moresi, L.-N., 1999. Some thoughts on the stability of cratonic lithosphere: Effects of buoyancy and viscosity. *J. Geophys. Res.* 104, 12747-12758.
- [16] McKinnon, W. B., 1999. Convective instability in Europa's floating ice shell, *Geophys. Res. Lett.* 26, 951-954.
- [17] Ozoe, H., Churchill, S.W., 1972. Hydrodynamic stability and natural convection in Ostwald-de Waele and Ellis fluids: The development of a numerical solution. *AIChE J.* 18, 1196-1206.
- [18] Palm, E., 1975. Nonlinear thermal convection. *Annu. Rev. Fluid Mech.* 7, 39-61.
- [19] Reese, C.C., Solomatov, V.S., Moresi, L.-N., 1999. Non-Newtonian stagnant lid convection and magmatic resurfacing of Venus. *Icarus*, 139, 67-80.
- [20] Reese, C. C., Solomatov, V. S., Baumgardner, J. R., 2002. Survival of impact-induced thermal anomalies in the Martian mantle, *J. Geophys. Res.* 107, 10.1029/2000JE001474.
- [21] Reynolds, R. T., Cassen, P. M., 1979. On the internal structure of the major satellites of the outer planets. *Geophys. Res. Lett.* 6, 121-124.

- [22] Schubert, G., Turcotte, D. L., Oxburgh, E. R., 1969. Stability of planetary interiors, *Geophys. J. R. Astr. Soc.* 18, 441-460.
- [23] Sleep, N. H., 2005. Evolution of the continental lithosphere, *Annu. Rev. Earth Planet. Sci.* 33, 369-393.
- [24] Solomatov, V.S., Scaling of temperature- and stress-dependent viscosity convection. *Phys. Fluids* 7, 266-274, 1995.
- [25] Solomatov, V. S., Barr, A. C. 2006. Onset of convection in fluids with strongly temperature-dependent, power-law viscosity. *Phys. Earth Planet. Inter.* 155, 140-145.
- [26] Solomatov, V. S., Barr, A. C. 2007. Numerical investigation of subcritical convection in strongly temperature-dependent viscosity fluids. *Phys. Fluids.*, submitted.
- [27] Solomatov, V. S., Moresi, L.-N., 2002. Small-scale convection in the D" layer, *J. Geophys. Res.* 107, 10.1029/2000JB000063.
- [28] Solomatov, V.S., Moresi, L.-N., 2000. Scaling of time-dependent stagnant lid convection: Application to small-scale convection on the Earth and other terrestrial planets. *J. Geophys. Res.* 105, 21795-21818.
- [29] Stengel, K.C., Oliver, D.C., Booker, J.R., 1982. Onset of convection in a variable viscosity fluid. *J. Fluid. Mech.* 120, 411-431.
- [30] Tien, C., Tsuei, H.S., Sun, Z.S., 1969. Thermal instability of a horizontal layer of non-Newtonian fluid heated from below. *Int. J. Heat Mass Transfer* 12, 1173-1178.

Table 1

$n$	$\exp(\theta)$	$Ra_{\text{cr}}^*$	$a_{\text{cr}}^*$	$Nu_{\text{cr}}^*$	$\Delta T_{\text{cr}}^*$
1	10	$2.94 \times 10^{-4}$	0.41	1.19	0.158
1	12	$5.61 \times 10^{-6}$	0.35	1.17	0.130
1	14	$9.77 \times 10^{-8}$	0.31	1.16	0.112
1	16	$1.58 \times 10^{-9}$	0.28	1.14	0.097
1	18	$2.43 \times 10^{-11}$	0.26	1.13	0.088
1	20	$3.57 \times 10^{-13}$	0.24	1.12	0.079
2	10	$2.90 \times 10^{-1}$	0.53	1.29	0.189
2	20	$1.81 \times 10^{-5}$	0.31	1.16	0.098
2	30	$5.50 \times 10^{-10}$	0.22	1.12	0.065
2	40	$1.23 \times 10^{-14}$	0.17	1.09	0.048
3	10	2.40	0.61	1.37	0.238
3	20	$5.49 \times 10^{-3}$	0.36	1.21	0.114
3	30	$6.80 \times 10^{-6}$	0.26	1.14	0.076
3	40	$6.42 \times 10^{-9}$	0.20	1.11	0.056
4	10	6.25	0.68	1.43	0.263
4	20	$8.62 \times 10^{-2}$	0.41	1.24	0.129
4	30	$6.77 \times 10^{-4}$	0.30	1.17	0.089
4	40	$4.15 \times 10^{-6}$	0.24	1.13	0.063

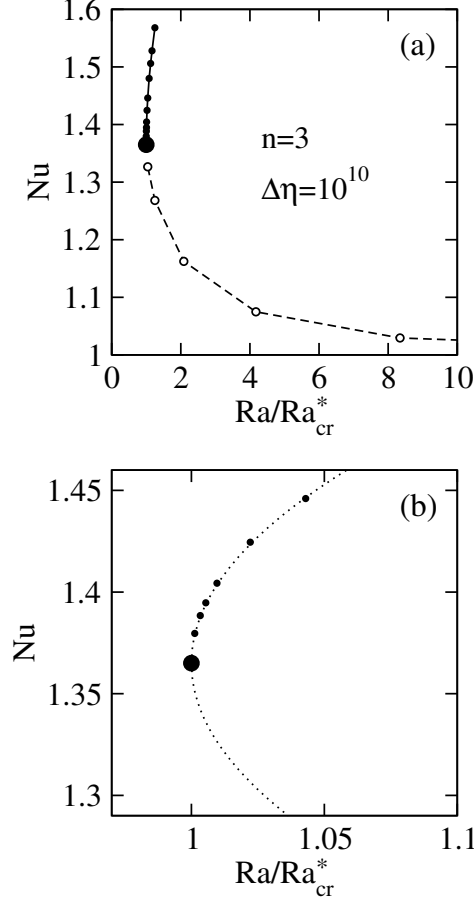


Fig. 1. (a) The Nusselt number as a function of Rayleigh number, normalized by the absolute minimum critical Rayleigh number,  $Ra_{cr}^*$  for  $n = 3$  and  $\Delta\eta = 10^{10}$ . The steady-state convection solutions are shown as circles connected by a solid line. The critical point is shown with a large solid circle. The Nusselt number,  $Nu = 1 + \xi(Nu_{cr}^* - 1)$ , of perturbations as a function of the critical Rayleigh number for the onset of convection (the “subcritical branch”), is shown with open circles connected by dashed line. (b) A zoomed view near the critical point. The expected parabolic fit  $Nu - Nu_{cr}^* \sim (Ra/Ra_{cr}^* - 1)^2$  near the critical point (Landau and Lifshitz 1987) is shown with a dotted line.

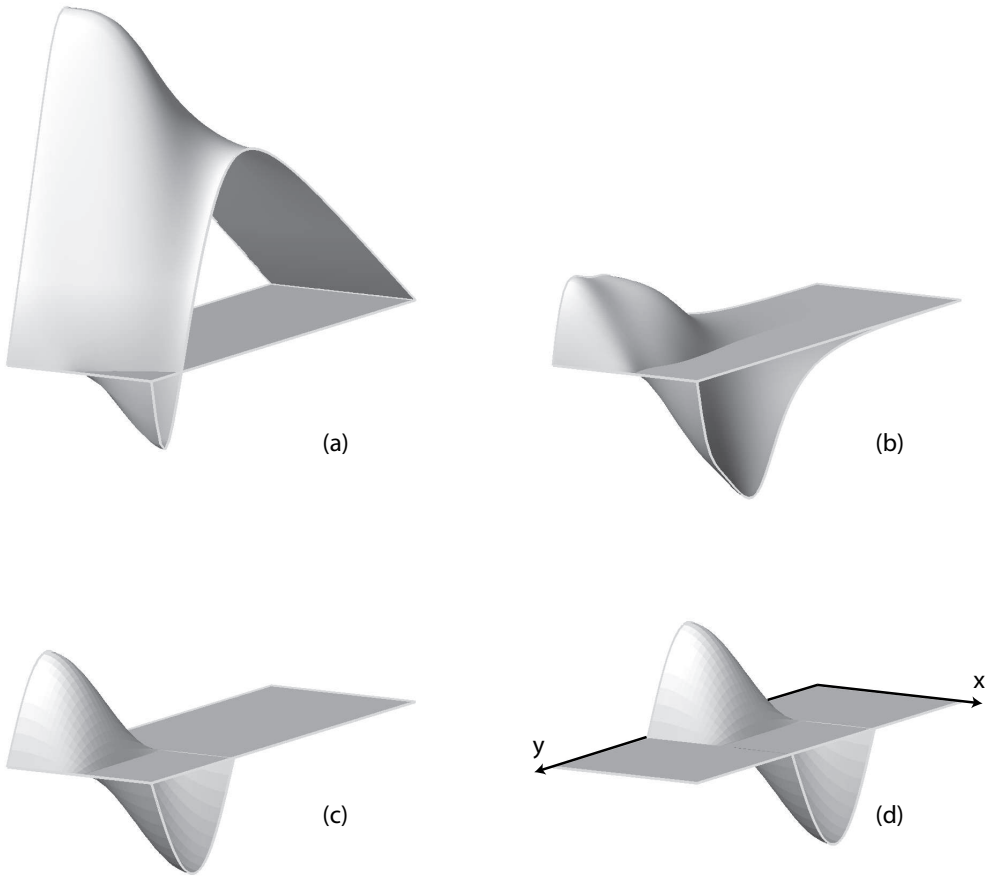


Fig. 2. Four finite amplitude temperature perturbations  $\delta T(x, y)$  used to initiate convection for  $n = 3$  and  $\exp(\theta) = 10^{20}$ . The temperature scale (vertical axis) is the same for all plots. (a) Here the perturbation is constructed using the temperature variation  $\delta T_{\text{cr}}^*(x, y) = T_{\text{cr}}^*(x, y) - y$  of the critical solution (at the absolute minimum critical Rayleigh number,  $Ra_{\text{cr}}^* = 5.5 \cdot 10^{-3}$ ) and reducing its amplitude by a factor of  $\zeta = 0.1$ ,  $\delta T(x, y) = \zeta \delta T_{\text{cr}}^*(x, y)$ . (b) Same as (a) but the horizontally averaged temperature is removed from the perturbation so that  $\int_0^a \delta T(x, y) dx = 0$ . (c) A simple harmonic perturbation is introduced at the bottom of the layer (the rheological sublayer), whose peak-to-peak amplitude is approximately the same as for (b). (d) The harmonic perturbation is shifted to the middle of the layer. The values of the critical Rayleigh number for the onset of convection are similar in the first three cases (0.054, 0.062 and 0.064 respectively), but in the last case it is one order of magnitude larger ( $\sim 0.61$ ).

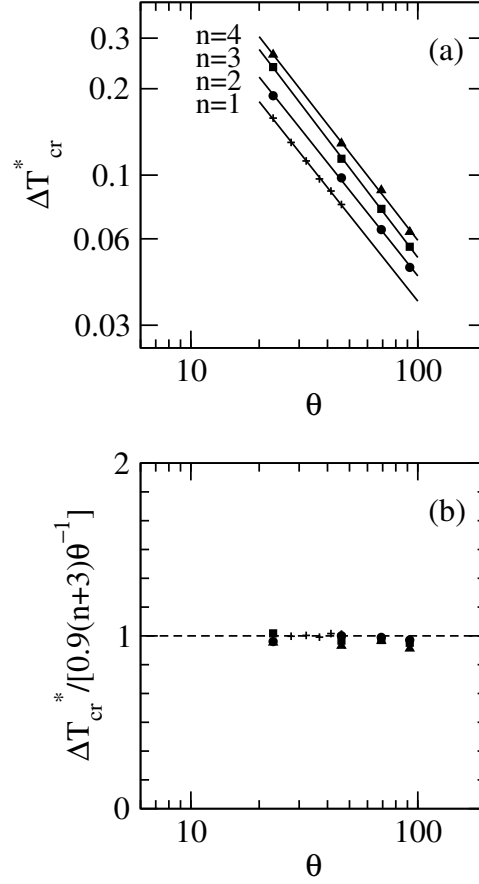


Fig. 3. (a) Dependence of the amplitude of the horizontal temperature difference,  $\Delta T_{cr}^*$ , at the absolute critical point on  $\theta$  for  $n = 1$  (open circles), 2 (circles), 3 (squares) and 4 (triangles). The slope of the fitting curves is -1 within 1 to 2% for all  $n$ . (b) The amplitude of the horizontal temperature difference,  $\Delta T_{cr}^*$ , normalized by  $0.9(n + 3)\theta^{-1}$ .

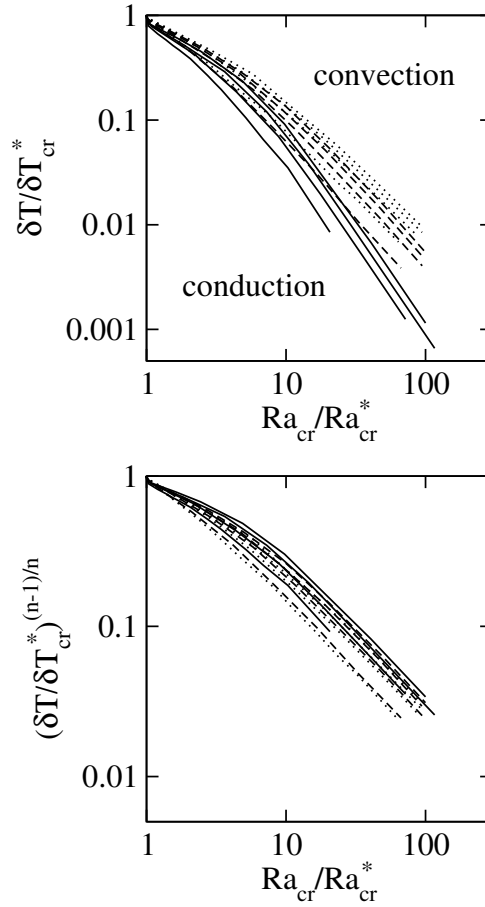


Fig. 4. (a) Summary of numerical constraints on the boundary between convection and conduction for finite initial perturbations:  $n = 2$  (solid line), 3 (dashed line) and 4 (dotted line). For each  $n$ , calculations were performed for  $\exp(\theta) = 10^{10}$ ,  $10^{20}$ ,  $10^{30}$  and  $10^{40}$  (the boundaries migrate upward with  $\theta$ ). The critical Rayleigh number,  $Ra_{cr}$  is normalized by its absolute minimum critical value  $Ra_{cr}^*$ . The temperature perturbation (relative to the conductive profile  $T_{\text{cond}} = z$ ) is normalized by the temperature perturbation at  $Ra = Ra_{cr}^*$  so that  $\delta T / \delta T_{cr}^* = 1$  at  $Ra_{cr} / Ra_{cr}^* = 1$ . (b) The same data are shown in axes  $Ra / Ra_{cr}^*$  and  $(\delta T / \delta T_{cr}^*)^{(n-1)/n}$ .

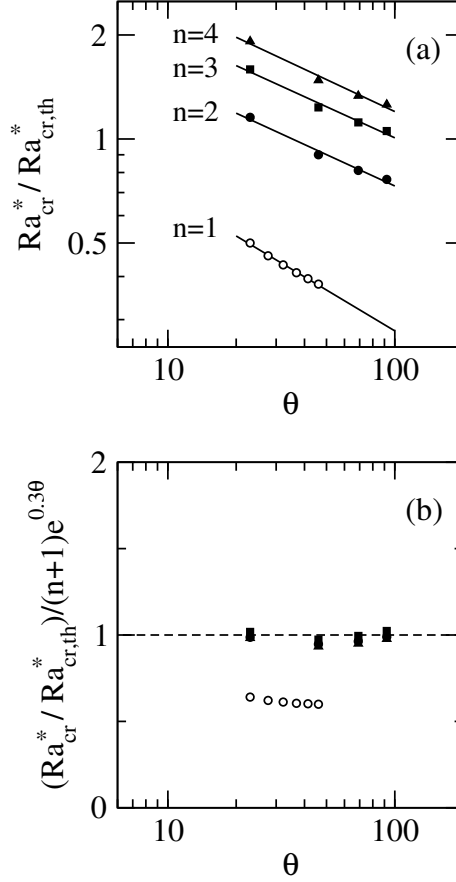


Fig. 5. (a) Ratio of the calculated absolute minimum critical Rayleigh number,  $Ra_{cr}^*$  to the theoretical value  $Ra_{cr,th}^*$  for  $n = 1$  (open circles), 2 (circles), 3 (squares) and 4 (triangles). The solid lines are the fitting curves:  $Ra_{cr}^* / Ra_{cr,th}^* = a\theta^{-b}$  with  $(a, b) = (1.7, 0.39), (2.9, 0.30), (4.0, 0.30), (5.0, 0.31)$  for  $n = 1, 2, 3$  and 4 respectively. (b) The ratio  $Ra_{cr,th}^* / Ra_{cr,th}^*$  normalized by  $(n + 1)\theta^{-0.3}$ .

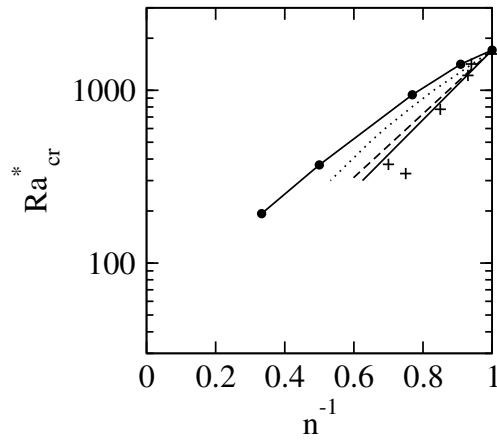


Fig. 6. Critical Rayleigh number for fluids with a solely stress-dependent viscosity, as a function of the power-law exponent  $n^{-1}$ . Solid circles connected by a solid line ( $n = 1.1, 1.3, 2$  and  $3$ ) are our results. Pluses corresponds to the the experimental data by Tien et al. (1969). The numerical results by Ozoe and Churchill (1972) are shown with a dotted line. The numerical results by Tien et al. (1969) are shown with a solid line (for two-dimensional rolls) and a dashed line (for hexagonal cells).

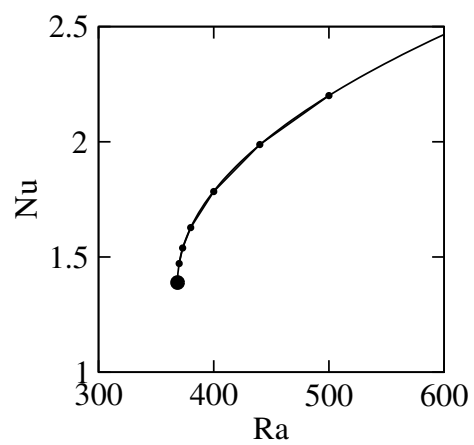


Fig. 7. The Nusselt number as a function of Rayleigh number near the critical point (small solid circles) for  $n = 2$  and  $\theta = 0$  (no temperature dependence). The parabolic fit is shown with a solid line. The critical point is shown with a large solid circle.